



# Major carbon losses from degradation of *Mauritia flexuosa* peat swamp forests in western Amazonia

Kristell Hergoualc'h · Jeffrey van Lent · Nelda Dezzee · Louis V. Verchot · Jan Willem van Groenigen · Mariela López Gonzales · Julio Grandez-Rios

Received: 15 February 2023 / Accepted: 1 June 2023  
© The Author(s) 2023

**Abstract** Tropical peat swamp forests are major global carbon (C) stores highly vulnerable to human intervention. In Peruvian Amazonia, palm swamps, the prevalent peat ecosystem, have been severely degraded through recurrent cutting of *Mauritia flexuosa* palms for fruit harvesting. While this can transform these C sinks into significant sources, the magnitude of C fluxes in natural and disturbed conditions remains unknown. Here, we estimated emissions from degradation along a gradient comprising undegraded (Intact), moderately degraded (mDeg) and heavily degraded (hDeg) palm swamps. C stock

changes above- and below-ground were calculated from biomass inventories and peat C budgets resulting from the balance of C outputs (heterotrophic soil respiration (Rh), dissolved C exports), C inputs (litterfall, root mortality) and soil CH<sub>4</sub> emissions. Fluxes spatiotemporal dynamics were monitored (bi)monthly over 1–3 years. The peat budgets (Mg C ha<sup>-1</sup> year<sup>-1</sup>) revealed that medium degradation reduced by 88% the soil sink capacity (from  $-1.6 \pm 1.3$  to  $-0.2 \pm 0.8$  at the Intact and mDeg sites) while high degradation turned the soil into a high source ( $6.2 \pm 0.7$  at the hDeg site). Differences stemmed from degradation-induced increased Rh ( $5.9 \pm 0.3$ ,  $6.2 \pm 0.3$ , and  $9.0 \pm 0.3$  Mg C ha<sup>-1</sup> year<sup>-1</sup> at the Intact, mDeg, and hDeg sites) and decreased C inputs ( $8.3 \pm 1.3$ ,  $7.1 \pm 0.8$ , and  $3.6 \pm 0.7$  Mg C ha<sup>-1</sup> year<sup>-1</sup> at the same sites). The large total loss rates ( $6.4 \pm 3.8$ ,  $15.7 \pm 3.8$  Mg C ha<sup>-1</sup>

Responsible Editor: Klaus Butterbach-Bahl.

**Supplementary Information** The online version contains supplementary material available at <https://doi.org/10.1007/s10533-023-01057-4>.

K. Hergoualc'h (✉) · J. van Lent · N. Dezzee · M. López Gonzales · J. Grandez-Rios  
Center for International Forestry Research (CIFOR) c/o Centro Internacional de la Papa (CIP), Av. La Molina 1895, Apdo Postal 1558, 15024 Lima, Peru  
e-mail: k.hergoualc'h@cifor-icraf.org

K. Hergoualc'h  
UMR Eco&Sols, Centre de coopération International en Recherche Agronomique pour le Développement (CIRAD), Montpellier, France

*Present Address:*  
J. van Lent · J. W. van Groenigen  
Soil Biology Group, Wageningen University and Research, Wageningen, The Netherlands

N. Dezzee  
Venezuelan Institute for Scientific Research (IVIC), Caracas, Venezuela

L. V. Verchot  
Center for International Tropical Agriculture (CIAT), Cali, Colombia

*Present Address:*  
J. Grandez-Rios  
Universidade Federal do Rio de Janeiro, Rio de Janeiro, Brazil

year<sup>-1</sup> under medium and high degradation), originating predominantly from biomass changes call for sustainable management of these peatlands.

**Keywords** Carbon budget · CO<sub>2</sub> emissions · Litterfall · Heterotrophic respiration · Palm swamp peatlands · Soil respiration

## Introduction

Tropical peat swamp forests are among the most carbon-dense ecosystems of the world and have been receiving a lot of attention because of the substantial role they can play in climate change mitigation strategies (Hergoualc'h et al. 2018; Murdiyarso et al. 2013). The largest areas of tropical peatlands are located in the lowland humid forests of South and Central America, Southeast Asia, and equatorial Africa (Gumbricht et al. 2017). Peruvian Amazonian lowland peatlands cover an area of 62,714 km<sup>2</sup> (Hastie et al. 2022) out of a total of 1,700,000 km<sup>2</sup> for the tropics (Gumbricht et al. 2017) and are mostly concentrated in the northeast Pastaza-Marañón River basin (43,617 km<sup>2</sup>). This peatland hotspot was estimated to store 4.1 Pg of carbon (C) in peat deposits up to 7.5 m deep (Hastie et al. 2022; Lähteenoja et al. 2012). In the region as elsewhere in lowland Amazonia, the main peat-forming ecosystem is a swamp forest dominated by the palm *Mauritia flexuosa* (locally named aguaje) that is regularly flooded by dynamic rivers such as the Amazon and its tributaries (Hergoualc'h et al. 2022; Draper et al. 2014). Other peat-forming ecosystems like herbaceous swamp and pole forest cover all together only 20% of the peatland surface (Hastie et al. 2022).

Though Peruvian Amazonian peatlands have not suffered extensive drainage and conversion as their Southeast Asian counterparts (Lilleskov et al. 2019), *M. flexuosa*-dominated swamps have been extensively degraded over the past four decades (Padoch 1988). The fruit of this palm is widely consumed for subsistence and commercial purposes, with a record entering the city of Iquitos of 8206 Mg in 2012–2013 (Horn et al. 2018). *M. flexuosa* fruits are primarily harvested by cutting down entire (female) palms leaving the trunks on the ground for palm weevils (*Rhynchophorus palmarum*) collection, a local food-source, and for building tracks to facilitate fruit transportation

through the flooded forest (Hergoualc'h et al. 2017a; Horn et al. 2012; Virapongse et al. 2017). While large-scale spatial assessments have not been conducted, this destructive harvesting practice is known to be widespread (Horn et al. 2018; Hidalgo Pizango et al. 2022). Notably a pilot study across a 3500 km<sup>2</sup> area along the Ucayali and Marañón River basins showed that 73% of palm swamps were degraded (Hergoualc'h et al. 2017a). Concerns about the ecological implications of this practice have been raised for many years (Padoch 1988; Penn et al. 2008) and include changes in forest structure and composition with a decline of *M. flexuosa* density (Bhomia et al. 2019; Hergoualc'h et al. 2017a) and the colonization of gaps by pioneer species when palms fail to regenerate (Bhomia et al. 2019). The potential for cascading consequences on biodiversity is also high as *M. flexuosa* plays an important role in the ecology and life cycle of numerous species (Bodmer et al. 1999). According to Hergoualc'h et al. (2017a), degradation in palm swamp peatlands translates into significant reductions in biomass with above and below-ground stocks (which average  $135.4 \pm 4.8$  Mg C ha<sup>-1</sup>) decreased by 11 and 17% following medium and high degradation, respectively. In addition, degradation was observed to alter the forest microclimate by increasing the air temperature (Hergoualc'h et al. 2020) and to induce changes in litterfall properties such as its nitrogen content and carbon-to-nitrogen (C:N) ratio (van Lent et al. 2019). Combined, these changes could stimulate organic matter mineralization, as suggested by results from in vitro peat incubations (van Lent et al. 2019). Higher soil heterotrophic respiration rates coupled with degradation-driven expected decreased organic matter inputs have the potential to increase net peat CO<sub>2</sub>-C emissions.

As per the IPCC, the net CO<sub>2</sub>-C uptake or emission rate of the peat is determined by the balance of organic matter inputs from litterfall and root mortality and outputs through heterotrophic soil respiration and soil carbon leaching (Drösler et al. 2014; Hergoualc'h and Verchot 2014). The peat net C gain or loss considers in addition peat CH<sub>4</sub> emissions which are typically an order of magnitude lower than CO<sub>2</sub> emissions in peatlands (Hergoualc'h and Verchot 2014; Griffith et al. 2020). In natural conditions, the peat C budget can alternate from sink to source with a long-term sink dominance leading to peat accumulation. In palm swamp peatlands of the Peruvian Amazonia

the historical accretion rate was estimated to average  $0.4 \text{ Mg C ha}^{-1} \text{ year}^{-1}$  based on radiocarbon dating (Lähteenoja et al. 2009a). The fluxes contributing to the peat C balance have not been investigated so far in Amazonian peatlands with research in the tropics almost exclusively confined to Southeast Asian peatlands. These fluxes are expected to be highly variable temporally depending on changes in the climate, plant phenology, and microbial activity (Griffiths et al. 2017). Notably, the El Niño southern oscillation (ENSO) induces large interannual rainfall fluctuations (Seneviratne et al. 2012) causing occasional floods in palm swamp peatlands for several months (Hergoualc'h et al. 2020; Roucoux et al. 2013). Fluxes can also be substantially spatially diverse, in particular root mortality, soil heterotrophic respiration and soil  $\text{CH}_4$  fluxes due to the heterogeneity of the forest floor. Most peat swamp forests present a hummock-hollow microtopography that influences the ecohydrological structure and biogeochemical processes including C dynamics (Jauhiainen et al. 2005; Graham et al. 2020; Hergoualc'h et al. 2020). A substantial portion of the large spatiotemporal variability of the fluxes can be explained by environmental and ecological variables notably the water table level and soil moisture, the structure of plant community, and the chemical composition of plant tissues and peat (Blodau 2002).

This study was carried out to assess ecosystem C losses associated with degradation in palm swamp peatlands of the Peruvian Amazonia. To do so, we conducted biomass inventories and monitored the components of the peat C budget along a degradation gradient that included one undegraded site and two sites of varying degradation level. We addressed the following research questions: (i) How much C is released from the ecosystem as a result of degradation? (ii) How are the peat  $\text{CO}_2\text{-C}$  and peat C budgets impacted by degradation? (iii) How do fluxes contributing to the peat C budget in particular soil respiration (total and heterotrophic) and litterfall vary in space and time under undegraded and degraded conditions? and (iv) How do environmental and ecological parameters control this variation?

## Materials and methods

### Site description

The study took place southwest of the city of Iquitos, in the Loreto region of the Peruvian Amazonia. According to 1948–1994 weather data, the climate is tropical humid with a mean annual temperature of  $27 \text{ }^\circ\text{C}$  and a mean annual rainfall of 3087 mm (Marengo 1998). There is no clear wet-dry season pattern with monthly precipitation rates typically in the range 100–300 mm throughout most of the year; monthly precipitations  $> 300 \text{ mm}$  are frequent in November, March and April, and less frequent between June and September (Marengo 1998).

We conducted the research in a 500 ha *M. flexuosa* swamp forest complex in and around the national park of Quistococha. According to paleoecological records, the forest started to develop about 1000 years ago and reached its current vegetation composition c. 400 years ago (Roucoux et al. 2013). The palm swamp is quasi-permanently waterlogged with a water table that rarely falls below 20 cm under soil surface (Hergoualc'h et al. 2020). The peat in the forest is classified as minerotrophic, i.e., nutrient-rich (Lähteenoja, et al. 2009b; van Lent et al. 2019) and reaches a depth of up to 5 m (Lähteenoja et al. 2009a).

We selected three 2-ha sites of varying levels of degradation inside the forest complex: an undegraded site hereafter referred to as Intact site, a moderately degraded site (mDeg) and a highly degraded site (hDeg) (Fig. 1a). Degradation in the context of this research refers to the cutting of *M. flexuosa* palms for fruit extraction and of trees. Levels of degradation (medium, high) were assigned upon visual inspection of the sites in situ and from remote sensing (Fig. S1) and informal interviews with community members on the intensity of palm and tree cutting. The Intact site (S  $03^\circ 49.949'$  W  $073^\circ 18.851'$ ) was situated within the Quistococha reserve, which has been protected since it was established a national park in 1984. The mDeg site (S  $03^\circ 50.364'$  W  $073^\circ 19.501'$ ) was located less than 2 km southwest of the Intact site, nearby the village of Las Brisas. The hDeg site (S  $03^\circ 48.539'$  W  $073^\circ 18.428'$ ) was less than 3 km northeast of the Intact site, at the border of the village of San Julian. Satellite images show that in 2010 the villages nearby the degraded sites did not exist

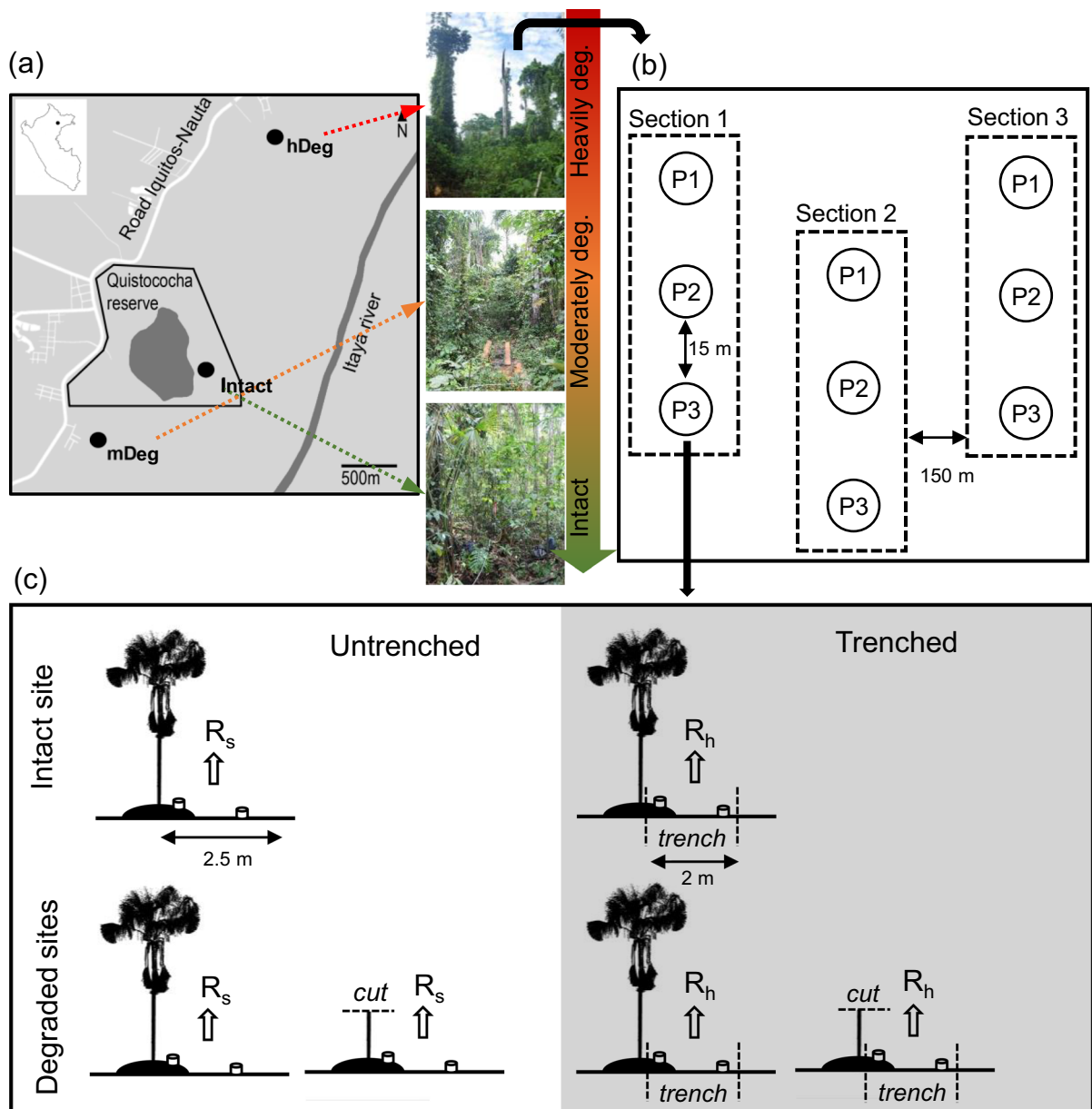


**Fig. 1** Location and pictures of the Intact, moderately (mDeg) and heavily (hDeg) degraded sites (a), layout of the experimental setup per site (b) and sketch of a plot (c). Each plot comprised an untrenched and a trenched treatment where total soil respiration ( $R_s$ ) and heterotrophic soil respiration ( $R_h$ ) were, respectively, monitored. Each treatment included one

subplot with a standing live palm at the Intact site and two subplots with a standing live palm and a cut palm at the degraded sites. Within each subplot, a distinction was made between hummock and hollow microtopographies. The *M. flexuosa* scan is from Caballero (2017)

yet and that the three sites were covered by a similar dense forest with closed canopy (S1). In 2016, the presence of the villages was associated with a reduced forest canopy that was more prominent at the hDeg site than at the mDeg site. According to an

inventory from 2015 (Bhomia et al. 2019) tree density at the Intact, mDeg and hDeg sites was 1846, 954 and 706 trees  $ha^{-1}$ , respectively, with predominantly broadleaf evergreen species. The density of *M. flexuosa* palms (with no male/female distinction) was 170,

164 and 16 stems  $\text{ha}^{-1}$  at the same sites. *M. flexuosa* was the dominant species at the Intact and mDeg sites according to Importance Value Index (IVI), while the hDeg site was dominated by the pioneer tree species *Cecropia membranacea* (Bhomia et al. 2019). Other tree species with high IVI included *Tabebuia insignis* (Intact site), *Vatairea* sp. (mDeg site) and *Hura crepitans* (hDeg site). Remnant *M. flexuosa* stumps were minimal at the Intact site (6 stumps  $\text{ha}^{-1}$ ) while both degraded sites presented a large number of *M. flexuosa* stumps (41  $\text{ha}^{-1}$  and 29  $\text{ha}^{-1}$  at the mDeg and hDeg sites) and logs. Peat depth was  $2.2 \pm 0.1$ ,  $> 2.65$  and  $1.0 \pm 0.2$  m at the Intact, mDeg and hDeg sites. The shallower peat at the hDeg site reflects the spatial variability in peat depth inside the forest complex rather than a legacy of degradation. Soil properties were mostly homogeneous among sites, with high concentrations of Ca and Mg, high percentage of base saturation and high phosphorus levels (Table S2). The pH of stagnant water was 5.9, 5.9, and 6.6 at the Intact, mDeg and hDeg sites (Bhomia et al. 2019).

#### Assessment of ecosystem level carbon emissions associated with degradation

Carbon emissions resulting from degradation were quantified over the period 2010–2015. For this, we considered the Intact site as a benchmark representative of ecological conditions at the mDeg and hDeg sites in 2010 when degradation based on satellite images can be assumed to have been negligible (S1). The space-for-time substitution approach we employed is an extensively used method which infers past trajectories from contemporary patterns and assumes that the observed differences can be attributed to land-use change and are not inherent to site differences (Blois et al. 2013). Emissions of C were computed from C stock losses in the aboveground biomass (AGB) and the peat as:

$$\text{Ecosystem C loss} = \text{AGB C loss} + \text{Peat C loss} \quad (1)$$

Changes in other C pools (belowground biomass, litter, and dead wood) are indirectly accounted for in peat C losses through their contribution of C inputs to the peat, as proposed by Hergoualc'h and Verhot (2011) (see detailed methods in the following Peat  $\text{CO}_2\text{-C}$  and C budget section).

Losses in AGB at the degraded sites were calculated from the difference in aboveground biomass C stock between the Intact site and the degraded sites in 2015 as:

$$\text{AGB C loss}_{\text{degraded site}} = (\text{AGB C}_{\text{Intact site}} - \text{AGB C}_{\text{degraded site}}) \quad (2)$$

where  $\text{AGB C}_{\text{Intact}} = 97.7 \pm 15.0$ ,  $\text{AGB C}_{\text{mDeg}} = 67.6 \pm 11.2$  and  $\text{AGB C}_{\text{hDeg}} = 36.8 \pm 10.5$   $\text{Mg C ha}^{-1}$  as from measurements by Bhomia et al. (2019).

Peat emissions were computed from the difference in C stock gained at the Intact site and C stock gained or lost at the degraded sites during 2010–2015 as:

$$\text{Peat C loss}_{\text{degraded site}} = |\text{Peat C}_{\text{gained Intact site}} - \text{Peat C}_{\text{gained/lost degraded site}}| \quad (3)$$

where the peat C stock gained/lost (see S3) was obtained from annual peat accumulation or loss rate (see next section Peat  $\text{CO}_2\text{-C}$  and C budgets). Peat accumulation at the Intact site was assumed to be in a steady state given the apparent absence of canopy changes in the mature forest during 2010–2016 (S1). At the degraded sites the peat was assumed to accumulate C in 2010 at a rate equal to the rate at the Intact site and to reach linearly the gain/loss rate measured in 2016. Assuming a linear change over a short-term period is a reasonable hypothesis in the absence of knowledge on annual dynamics of peat accumulation or loss rate in tropical peat swamp forests.

#### Peat $\text{CO}_2\text{-C}$ and C budget in undegraded and degraded conditions

The peat  $\text{CO}_2\text{-C}$  budget, i.e. the net emission or removal of  $\text{CO}_2\text{-C}$  from the soil as defined by the IPCC (Drösler et al. 2014), includes on- and off-site C fluxes and was computed as:

$$\text{Peat } \text{CO}_2\text{-C budget} = (\text{Rh} + \text{DOC}) - (\text{Litterfall} + \text{Root mortality}) \quad (4)$$

where peat  $\text{CO}_2\text{-C}$  budget is the net emission or removal of  $\text{CO}_2\text{-C}$  from the soil; Rh is the soil heterotrophic respiration; DOC is the dissolved organic carbon exported from the soil; litterfall is the above



ground input of C through litterfall; and root mortality is the below ground input of C from root mortality. All components are expressed in  $\text{Mg C ha}^{-1} \text{ year}^{-1}$ . A positive budget indicates that the peat is a net source of C to the atmosphere.

Furthermore, the peat C budget i.e. the net gain or loss of carbon from the soil was calculated following the IPCC guidelines (Blain et al. 2014) as:

$$\text{Peat C budget} = \text{Peat CO}_2\text{-C budget} + \text{soil CH}_4\text{-C} \quad (5)$$

where soil  $\text{CH}_4\text{-C}$  is the flux of methane from the soil in  $\text{Mg C ha}^{-1} \text{ year}^{-1}$ .

The budgets were based on cumulative or average flux rates in c. April 2016–March 2017 (see Y2 in S4) when these were monitored concomitantly across the sites. Soil heterotrophic respiration and litterfall rates were measured as part of this study (see next section). Root mortality rates were measured monthly at the sites by Dezzio et al. (2021) from March 2016 to January 2017. The DOC loss was assigned the default IPCC value for natural flux in undrained tropical peatlands (Drösler et al. 2014) as no such data were available for the sites. Soil  $\text{CH}_4$  fluxes were monthly monitored by Hergoualc'h et al. (2020) concomitantly with soil respiration measurements (S4).

#### Soil respiration, litterfall, litter decomposition and environmental parameters

Soil respiration, litterfall, litter decomposition and environmental parameters were studied along three 250  $\text{m}^2$  sections per site separated by ~150 m (Fig. 1b). Within each section, we set up three plots ~15 m from each other. Monitoring followed a protocol specific to each component (litterfall, soil respiration, environmental variables) which is detailed in the subsections below and in S5 (methods and results for environmental parameters). Measurements started in May 2014 and ended in July 2018 with lags between sites due to research permission procurement, among other factors. Annual results were computed for the periods April 2015–March 2016 (Y1), April 2016–March 2017 (Y2), and April 2017–March 2018 (Y3) when monitoring overlapped across sites (S4).

#### Litterfall and litter decomposition

We monitored small- and large-size litterfall. Small-size litter included leaves, reproductive parts, and fine twigs; large-size litter encompassed *M. flexuosa* fronds, trunks, and tree branches. Large-size litterfall was measured bimonthly from June 2016 (S4) in one 5×5 m quadrant per section for a total of three site-replicates. The quadrant was cleared of debris at the onset of the experiment and upon each litter collection. The litter was weighed in situ and its dry mass was computed from the dry-to-wet ratio of one sample per component (*M. flexuosa* frond, trunk, and tree branch) dried at 60 °C to constant mass at each sampling time. Small-size litterfall was monitored monthly starting July 2014 (S4) in triplicate and quadruplicate litter traps per plot at the Intact and degraded sites, respectively, for a total of 27 and 36 replicates at the same sites. Small-size litterfall was captured in 0.09  $\text{m}^2$  traps installed randomly about 1 m above the soil. Upon collection, litter samples were oven-dried at 60 °C to constant mass, weighed, milled and homogenized. The C content of the tree leaf and branch, and *M. flexuosa* frond was measured from triplicate samples per site by the induction furnace method (Costech EA C–N Analyzer). The C concentration of *M. flexuosa* trunks was assumed to be similar to that of tree branches. Annual litterfall rates were computed by annualizing (bi)monthly average rates and were site-scaled using the proportional density of live trees and live *M. flexuosa* relative to their density at the Intact site (Table S6A). These densities were obtained from a vegetation inventory which methods and results are presented in S6.

Litter decomposition was studied over 1.5 years (July 2015–January 2017) using triplicate litter bag per section for a total of nine replicates per site and sampling time. Undecomposed leaves undifferentiated by species were randomly collected from freshly fallen litter on the forest floor, and moist samples of a 3 g dry mass equivalent were placed in 15×15 cm decomposition bags constructed of fiberglass mesh (openings 0.75×0.75 mm). At each site, 72 bags were randomly installed on the soil surface and nine bags were collected 12, 41, 73, 110, 189, 272, 460 and 560 days later. Upon collection bags were gently rinsed with distilled water, oven dried at 60 °C to constant mass, and weighted. The rate of decomposition

was determined by regression analysis of the remaining dry mass against time:

$$Y_t / Y_0 = \exp^{-kt} \quad (6)$$

where  $Y_t/Y_0$  is the percentage ratio of remaining dry mass at time  $t$  (days) to initial dry mass  $Y_0$  and  $k$  is the decay rate constant ( $\text{day}^{-1}$ ).

### Soil respiration

We measured total soil respiration (Rs) and heterotrophic soil respiration (Rh) in, respectively, an untrenched treatment and a trenched treatment established in each plot (Fig. 1c). For both treatments, we used a stratified sampling design that accounted for *M. flexuosa* palm status (live and cut) and soil microtopography (hummock and hollow). Given the absence of degradation at the Intact site, soil respiration was monitored only around live *M. flexuosa* palms. At the degraded sites, Rh measurements around cut palms were expected to capture the decomposition of dead thick roots of *M. flexuosa* stumps in addition to the decomposition of above ground litter and soil organic matter (SOM).

Inside the  $2.5 \times 2.5$  m subplots that included either a standing live palm or a cut palm sampling in hummocks was performed  $< 0.5$  m away from the palm trunk in the main rooting zone and sampling in hollows was conducted  $> 1.5$  m from the same trunk outside the main rooting zone. In the trenched treatment, trenches were cut to 1.5 m deep and 0.5 m wide around a subplot of  $2 \times 2$  m. Preliminary soil coring showed that roots beyond 1.5 m depth were minimal. To prevent roots from growing into the trenches, the inner walls of the trenches were covered with six layers of construction plastic and backfilled. Recruitment of new vegetation in the quadrant was prevented through monthly seedling removal. When the experiment was uninstalled in August 2018 no live roots were found inside the trenched quadrants.

Soil respiration was measured monthly from May 2014 (S4) using the dynamic closed chamber method. We used a portable infrared gas analyzer (EGM-4, PP systems, USA) connected to a soil respiration chamber (SRC-1) (PP System, Amesbury, USA). The analyzer was equipped with a drierite filter ( $\geq 98\%$   $\text{CaSO}_4$  and  $\leq 2\%$   $\text{CoCl}_2$ ) to reduce the air humidity. The chamber was placed on top of opaque PVC

collars (10 cm diameter, 10 cm height) that had been permanently installed 3–5 cm into the soil one month before starting the measurements. Collars were manually fanned before closure and the  $\text{CO}_2$  concentration was recorded automatically every 4.8 s for about 2–3 min following closing. The  $\text{CO}_2$  flux was calculated from the linear increase of the concentration over time. Boardwalks were constructed at the onset of the experiment to access sampling points without creating disturbance.

Monthly average Rs and Rh rates per palm status (live or cut) and microtopography (hummock and hollow) were calculated from the nine replicate plots per site. Soil respiration was not measured between April and June 2015 due to flooding caused by the 2015 El Niño event, and in August 2015, March 2016, May 2017 and August 2017 due to logistical problems. Corresponding missing Rs rates were imputed with values estimated from linear regressions between Rs rates measured with the infrared gas analyzer and Rs rates measured by gas chromatography [concomitantly with  $\text{CH}_4$  and  $\text{N}_2\text{O}$  fluxes as described in the paper by Hergoualc'h et al. (2020)] (S7).

Annual respiration rates were computed by linear interpolation (or trapezoidal integration) between measurement dates and were site-scaled considering the relative proportions of hummocks and hollows around live and cut palms (Table S6B). Soil respiration around trees which did not form hummocks was not monitored and was assumed to be similar to soil respiration in hollows around palms.

### Statistics

Statistical analysis was performed using R software (Core Team R 2017) and PRIMER v7 (Anderson 2017) for soil respiration, and IBM SPSS Statistics for Windows 25.0 (IBM Corp. 2017) for all other analysis, setting a statistical significance level at 5%. The potential effects of disturbance level (i.e., site: Intact, mDeg and hDeg), status (live vs. cut palm), microtopography (hummock vs. hollow), and temporal variability (40 months; i.e., the overlapping period across sites) on Rh and Rs were examined using a mixed-effects ANOVA model with four factors. Sampling month was treated as a random factor while disturbance level, status, and microtopography were treated as fixed effects. The design was asymmetric

because not all status levels were present at all sites (specifically, there were no cut palms at the Intact site), and it was unbalanced because not all combinations of treatments had nine replicates per sampling month (due to missing data). Considering these limitations, adequate degrees of freedom, mean squares, and F-ratio were calculated using the PERMANOVA routine in PRIMER v7. Even though this method was specifically designed for multivariate data, it can be used for univariate data using Euclidean distance (Anderson 2017). Its advantage is that it properly handles asymmetrical and unbalanced designs. In addition, as residuals were generally not normally distributed, the ANOVA using the traditional tabulated F values would have been inappropriate. Therefore, the probability associated to each empirical F-ratio was estimated using 9999 permutations of the residuals under the reduced null model. Normality of residuals was tested using the Shapiro Wilk test, and visual interpretation of Q-Q plots; the homogeneity of variances was verified using the Levene's test.

The non-parametric Wilcoxon and Kruskal–Wallis tests were used for, respectively, single and multi-comparison of litterfall and litter decomposition data given the non-normal distribution of their residuals.

Relationships between respiration rates, litterfall rates and environmental variables were examined with linear and non-linear, simple and multiple regression analysis using the entire dataset (May 2014–July 2018). To identify the best predictors of soil respiration along the forest complex, we tested relationships using monthly averages from all sites and binned them into classes for the independent variables (e.g. 10 cm WT, 10% WFPS). We also assessed relationships between the three-year mean annual soil heterotrophic respiration rates and soil properties (Table S2) considering the microtopography around live palms. Respiration rates around cut palms were not included in this assessment since soil samples were collected around live palms.

The Gaussian error propagation method was used for propagating uncertainties of monthly averages and computing the standard error of annual rates. This method is suitable for step-by-step calculations intended to compute ecological quantities that are expressed as an analytical equation using addition, subtraction, multiplication and division, such as C stocks or fluxes (Lo 2005). Site-scale annual or average values and peat  $\text{CO}_2\text{-C}$  and C budgets  $\pm$  standard

error which did not overlap were considered significantly different between sites/years. Results are presented as mean or cumulative values  $\pm$  standard error.

## Results

### Litterfall and litter decomposition

Tree leaf litterfall ranged from a low 0.09 to a high 1.14 Mg C ha<sup>-1</sup> month<sup>-1</sup> and was the dominant component of litterfall (Fig. 2a). Following the El Niño flooding that took place from April to June 2015, a significant amount of tree leaves fell at the Intact and mDeg sites. High peaks in leaf fall also occurred at the three sites between November 2015 and May 2016. *M. flexuosa* frond- and tree branch-fall varied in a narrow range (from 0.00 to 0.24 Mg C ha<sup>-1</sup> month<sup>-1</sup>) with no specific temporal trend. The fall of palm trunk only occurred at the hDeg site in the months of August 2016 and June 2017 and represented very low C inputs (0.04 and 0.05 Mg C ha<sup>-1</sup> month<sup>-1</sup>, respectively). Monthly tree leaf litterfall was not correlated with either the precipitation rate or the WT level of the month or of the preceding month.

Site-scale tree leaf litterfall was higher in year 1 than in year 3 ( $P=0.036$ , 0.010, and 0.018 at the Intact, mDeg, and hDeg sites, respectively) (Fig. 2b) and tended to increase with higher precipitation (S8). Site-scale large-size litterfall (tree branch, *M. flexuosa* frond and trunk) was similar in year 2 and year 3 at all sites ( $P>0.307$ ). Every year and over the 3 years, site-scale litterfall was lower at the hDeg site than at the Intact and mDeg sites.

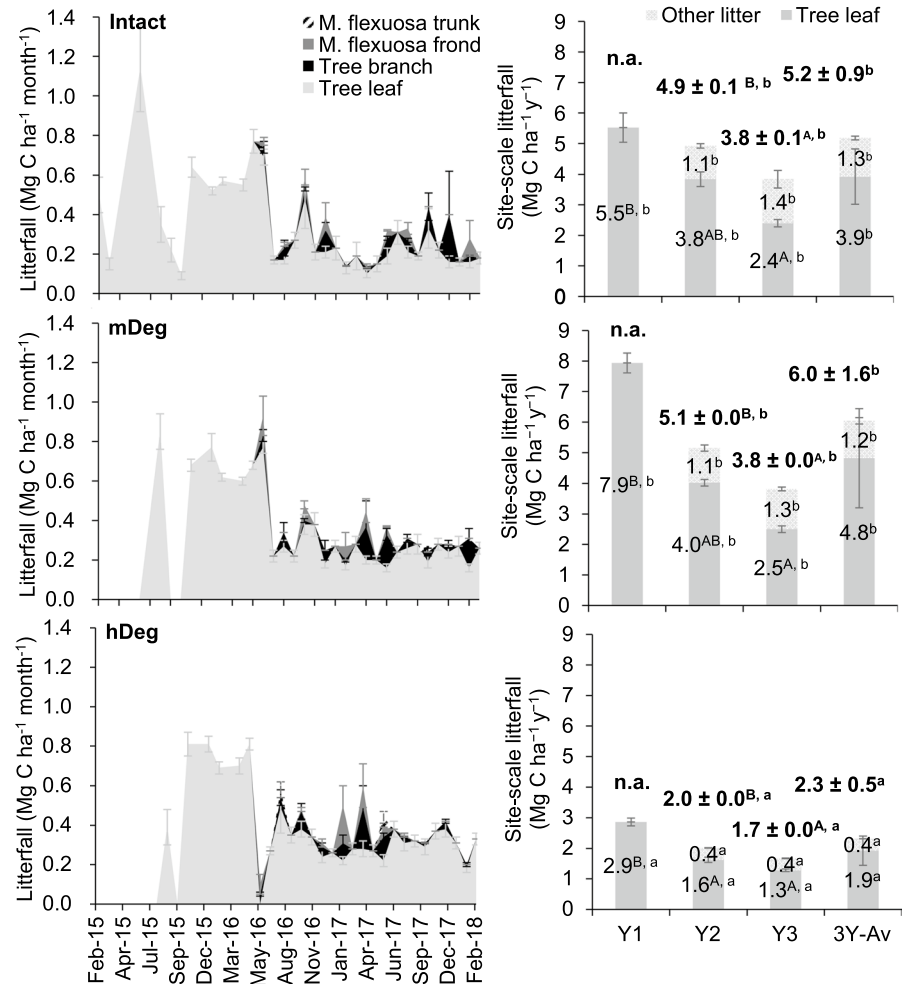
Leaf decomposition in situ was fast with only  $24.8 \pm 2.3\%$  of mass remaining after 560 days on average (Fig. S9). According to the exponential decay rate models, the half-life of the litter was 242, 196, and 301 days at the Intact, mDeg, and hDeg sites, respectively. Mean leaf decay was faster at the mDeg site ( $k=0.0032 \pm 0.0002 \text{ day}^{-1}$ ) than at the Intact site ( $k=0.0027 \pm 0.0002 \text{ day}^{-1}$ ) and at the hDeg site ( $k=0.0021 \pm 0.0002 \text{ day}^{-1}$ ) ( $P<0.0001$ ).

### Soil respiration

Monthly average  $R_s$  rates fluctuated over a wide range (7.5 to 124.5 kg C ha<sup>-1</sup> day<sup>-1</sup>) with no



**Fig. 2** (Bi)monthly (a, stacked values) and annual (b) average litterfall rates at the Intact, moderately degraded (mDeg), and heavily degraded (hDeg) sites. Error bars are SE. Site-scale annual rates are presented for tree leaf, other litter and in total in Y1 (April 2015–March 2016), Y2 (April 2016–March 2017), Y3 (April 2017–March 2018). Differences in litterfall between years within a site are indicated by uppercase letters. Differences between sites within a year or for the 3-year annual mean (3-Y mean) are indicated by lowercase letter



distinctive common pattern across sites (Fig. 3a). The rates decreased exponentially with increasing WFPS (Fig. 4a) and decreased linearly with increasing WT (Fig. 4b). Annual Rs rates were the lowest in year 2 (Fig. 3a) and were higher in hummocks than in hollows across the 3 years (Fig. 3b). In all years, annual Rs rates varied among sites in the order Intact > hDeg > mDeg (Fig. 3a).

Monthly average Rh rates varied between 3.6 and 78.3 kg C ha<sup>-1</sup> day<sup>-1</sup> with no common temporal trend across sites (Fig. 3c) and decreased linearly as the WFPS rose (Fig. 4c). Annual Rh rates were higher in year 3 than in year 1 at all sites (Fig. 3c) and were similar among microtopographies across the 3 years (Fig. 3d). At the degraded sites, annual Rh rates over the 3 years were generally higher around live palms than around cut palms, at a same microtopography (Fig. 3d). They were higher at the hDeg site than at

the other two sites (Fig. 3d). Around live palms, they decreased significantly with increasing peat C:N ratio, C content (Fig. 4d), NH<sub>4</sub><sup>+</sup> concentration and P content (Fig. 4e) and increased as peat Ca content got higher (Fig. 4f). Finally, the Rh to Rs ratio was significantly higher at the mDeg (0.94 ± 0.06) and hDeg sites (0.87 ± 0.05) than at the Intact site (0.54 ± 0.04) (P < 0.0001).

Peat CO<sub>2</sub>-C and C budget and C emissions from degradation

At all sites, C outputs from the soil occurred largely through heterotrophic respiration while C inputs were predominantly organic matter from aboveground litterfall (Table 1). The peat C budgets were similar to the peat CO<sub>2</sub>-C budgets due to minimal soil CH<sub>4</sub> emissions as compared to most other CO<sub>2</sub>-C

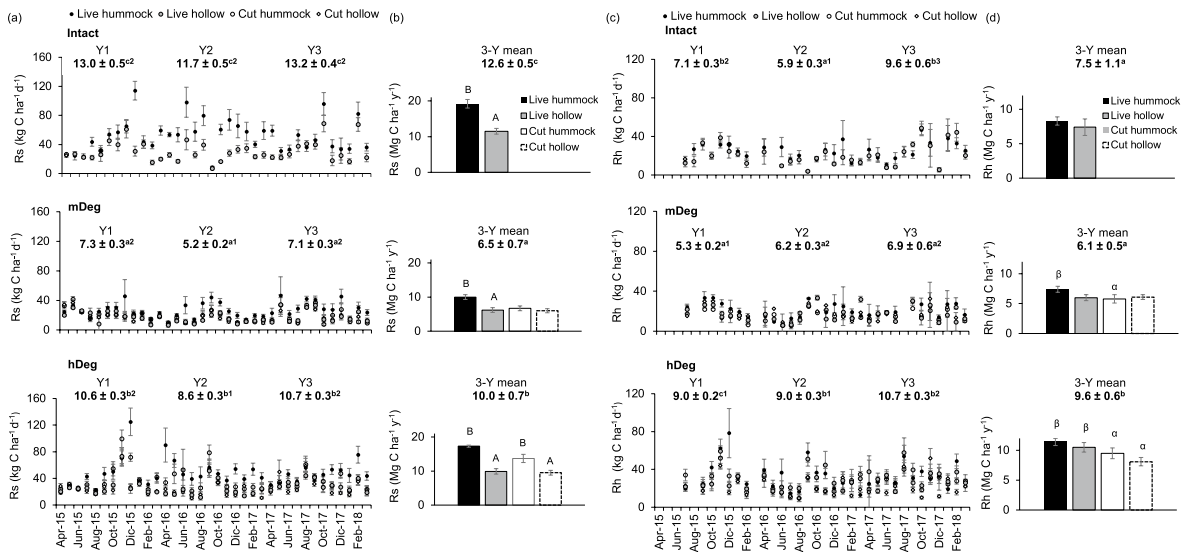


**Fig. 3** Monthly mean and annual soil respiration (Rs) rates (a) and soil heterotrophic respiration (Rh) rates (c) at the Intact, moderately (mDeg) and heavily (hDeg) degraded sites. Error bars are SE. Monthly means are presented per palm status and spatial position ( $n=9$ ). Site-scale annual rates are cumulative values in Y1 (April 2015–March 2016), Y2 (April 2016–March 2017) and Y3 (April 2017–March 2018). Three-year annual Rs means (b) and Rh means (d) are presented per palm

status and spatial position and at site-scale. Lower case letters indicate significant differences between sites. Numbers indicate significant differences between years within a site. Capital letters indicate significant differences between microtopographies within a site. Greek letters indicate significant differences between status (live, cut) within a microtopography at the degraded sites. No letters or numbers are displayed in the absence of a significant difference

fluxes. These budgets indicate that medium degradation reduced by 88% the C sink capacity of the soil (from  $-1.6 \pm 1.3$  Mg C ha<sup>-1</sup> year<sup>-1</sup> at the Intact site to  $-0.2 \pm 0.8$  Mg C ha<sup>-1</sup> year<sup>-1</sup> at the mDeg site) and high degradation turned the soil into a high net C source ( $6.2 \pm 0.7$  Mg C ha<sup>-1</sup> year<sup>-1</sup> at the hDeg site). Our estimates suggests that over the 5-year observation period (2010–2015), the peat C stock gained  $7.9 \pm 3.3$  and  $6.0 \pm 2.9$  Mg C ha<sup>-1</sup> at the Intact and mDeg sites, respectively, resulting in a net loss of  $1.9 \pm 4.4$  Mg C ha<sup>-1</sup> following medium degradation (Table 1). Over the same period, the net loss from high degradation amounted to  $17.8 \pm 4.3$  Mg C ha<sup>-1</sup>.

Peat and aboveground biomass C stock losses (Table 1) resulted in an average net loss rate of  $6.4 \pm 3.8$  and  $15.7 \pm 3.8$  Mg C ha<sup>-1</sup> year<sup>-1</sup> for medium and high degradation, respectively. Ecosystem losses stemmed essentially from AGB stock changes but the contribution of the peat to the total increased with degradation intensity from 6% at the mDeg site to 23% at the hDeg site.

## Discussion

Spatio-temporal variation and controls of the components of the peat C budget (litterfall, soil heterotrophic respiration) along the degradation gradient

Plant litter is the primary source of peat and its slow decomposition rate is fundamental for peat accumulation (Chimner and Ewel 2005; Laiho 2006). We found that tree leaves contributed the main proportion of total litterfall (75–83%) in agreement with observations in tropical evergreen forests (Zhang et al. 2014) and in peat swamp forests of Micronesia (Chimner and Ewel 2005). Litterfall did not follow a clear temporal pattern probably due to the low intra-annual climate seasonality at the sites, which corroborates similar findings by Ong et al. (2015) in a Malaysian peat swamp forest with a relatively aseasonal climate. Notwithstanding, inter-annual variability was important with notably high tree leaf fall rates in year 1 (Fig. 2b) induced by the El Niño-related flooding from April to June 2015 and subsequent

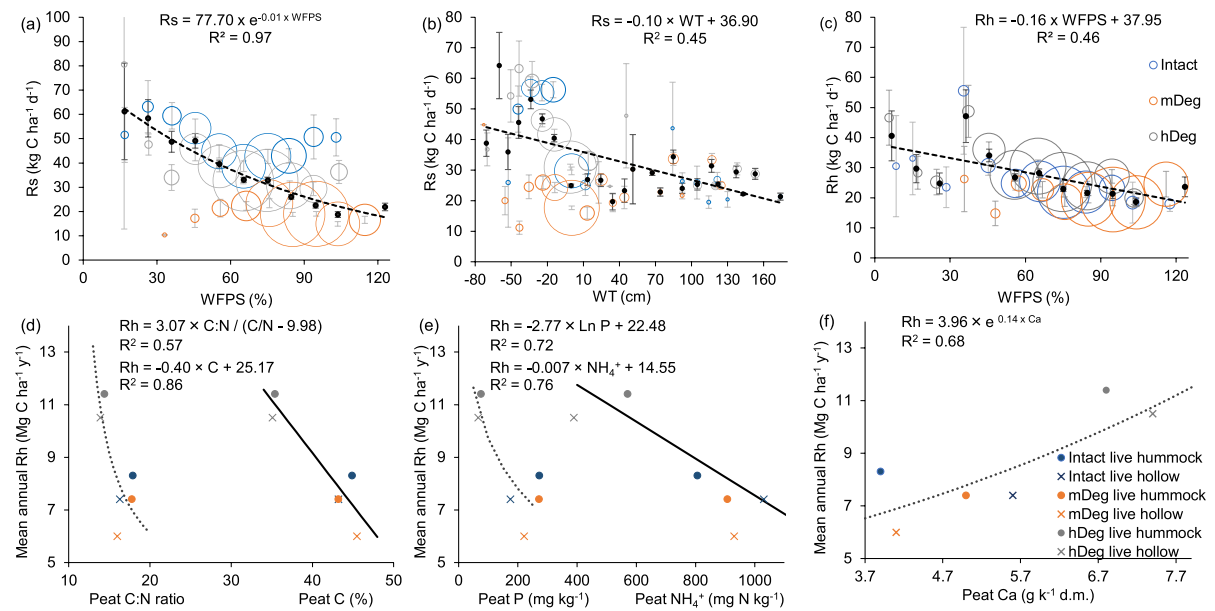


**Fig. 4** Relationship between monthly average ( $R_s$ ) rates and the soil water-filled pore space (WFPS) (a) and water table level (WT) (b), and monthly average ( $R_h$ ) rates and the soil water-filled pore space (WFPS) (c). Relationships between 3-year annual mean soil heterotrophic respiration ( $R_h$ ) and mean soil properties of hummocks and hollows with live palms at the Intact, moderately degraded (mDeg), and heavily

degraded (hDeg) sites (d–f). Monthly emissions were binned into 10% WFPS and 10 cm WT intervals, disaggregated by site (bubbles) and all sites combined (black dots). Bars are SE and the size of the bubbles is relative to the sample size. Models between monthly respiration rates from all sites or 3-year annual mean  $R_h$  rates and variables (dashed black or grey lines and plain black lines) are presented

high precipitation rates that persisted until March 2016 (Fig. S5A). Post-flooding litterfall peaks evidence a dieback of woody tree leaves possibly caused by sustained stomatal closure and production of phytotoxic compounds during prolonged anoxic conditions (Kozłowski 1997; Pezeshki 2001). The tendency towards higher annual tree leaf fall with increased annual precipitation (Fig. S8) concurs with findings by Tonin et al. (2017) of a positive and strong control of precipitation over plant litter dynamics in tropical forests of Brazil. According to the existing literature (Bhomia et al. 2019; Mishra et al. 2004), disturbance tends to reduce the structural and compositional complexity of forests which in turn affects the quantity and quality of litterfall, among other ecosystem functions. Our results show that litterfall at the highly degraded site decreased by 56% as compared to the Intact site. This finding is consistent with general understanding on the impacts of forest degradation on plant productivity (e.g., Giweta 2020; Kerdraon et al. 2020; Seta et al. 2018) and is slightly higher than the 42% reduction observed in degraded peat swamp

forests of Southeast Asia as compared to undegraded forests (Hergoualc’h and Verchot 2014). In terms of magnitude, the 3-year average total litterfall at the Intact site ( $5.2 \pm 0.9$  Mg C ha<sup>-1</sup> year<sup>-1</sup>) is within the range assessed for Southeast Asian undisturbed peat forests ( $7.4 \pm 0.7$  Mg C ha<sup>-1</sup> year<sup>-1</sup>; Hergoualc’h and Verchot 2014) and for flooded forests of South America after correction for large branch fall inclusion ( $4.5 \pm 0.7$  Mg C ha<sup>-1</sup> year<sup>-1</sup> without large branch fall; Chave et al. 2010). Our values, however, are higher than those reported for preserved and degraded palm swamps of the Cerrado in the Southeast of Brazil ( $2.8$  to  $3.8$  Mg dry matter ha<sup>-1</sup> year<sup>-1</sup>) (Sales et al. 2020) which can be explained by the low tree cover of these swamps (5–10%; Gonçalves et al. 2021).

Leaf litter decomposition was the fastest at the moderately degraded site and the slowest at the heavily degraded site (Fig. S9). Since lower C:N ratios usually favor litter decomposition (Krishna and Mohan 2017) and leaf litter C:N ratio declined along the degradation gradient ( $33.9 \pm 0.2$ ,  $32.1 \pm 0.1$  and  $25.6 \pm 3.3$  at the Intact, mDeg, and hDeg sites,

**Table 1** Peat CO<sub>2</sub>-C and peat C budget at the Intact, moderately degraded (mDeg) and heavily degraded (hDeg) sites and ecosystem C loss resulting from degradation over the period 2010–2015

	Intact	mDeg	hDeg	Intact-mDeg	Intact-hDeg
<b># Carbon fluxes (Mg C ha<sup>-1</sup> year<sup>-1</sup>)</b>					
<b>Soil C outputs</b>					
Rh	5.9 <sup>a</sup> ± 0.3	6.2 <sup>a</sup> ± 0.3	9.0 <sup>b</sup> ± 0.3		
DOC	0.6 ± 0.0	0.6 ± 0.0	0.6 ± 0.0		
<b>Soil C inputs</b>					
Litterfall	4.9 <sup>b</sup> ± 0.1	5.1 <sup>b</sup> ± 0.0	2.0 <sup>a</sup> ± 0.0		
Root mortality	3.4 ± 1.3	2.0 ± 0.8	1.5 ± 0.7		
<b>Peat CO<sub>2</sub>-C budget</b>	<b>-1.8<sup>a</sup> ± 1.3</b>	<b>-0.3<sup>a</sup> ± 0.8</b>	<b>6.0<sup>b</sup> ± 0.7</b>		
Soil CH <sub>4</sub> emission	0.21 <sup>c</sup> ± 0.01	0.11 <sup>a</sup> ± 0.02	0.18 <sup>b</sup> ± 0.02		
<b>Peat C budget</b>	<b>-1.6<sup>a</sup> ± 1.3</b>	<b>-0.2<sup>a</sup> ± 0.8</b>	<b>6.2<sup>b</sup> ± 0.7</b>		
<b>§C stocks or stock changes (Mg C ha<sup>-1</sup>)</b>					
Peat stock gained/lost (5 year <sup>-1</sup> )	-7.9 ± 3.3	-6.0 ± 2.9	9.9 ± 2.8	1.9 ± 4.4	17.8 ± 4.3
AGB stock	97.7 ± 15.0	67.6 ± 11.2	36.8 ± 10.5	30.1 ± 18.7	60.9 ± 18.3
<b>Ecosystem loss</b>				<b>32.0 ± 19.2</b>	<b>78.7 ± 18.8</b>

A negative value represents an uptake of C. The peat CO<sub>2</sub>-C budget results from the difference of soil C outputs and C inputs in year 2 (April 2016–March 2017) when all fluxes were monitored concomitantly. The peat C budget includes CH<sub>4</sub>-C emissions measured in year 2. Ecosystem loss from the peat and aboveground biomass (AGB) was computed as the difference of stock between the Intact site and the degraded sites. Values are average ± standard error

<sup>#</sup>C outputs from heterotrophic respiration (Rh) are from this study, loss as dissolved organic carbon (DOC) is the default IPCC value (Drösler et al. 2014). C inputs from litterfall are from this research, inputs from root mortality are also site-specific (Dezzeo et al. 2021). The soil CH<sub>4</sub> emission was measured at the sites (Hergoualc'h et al. 2020)

<sup>§</sup>Peat C stock gained/lost per site are presented in SI2 and ABG was measured by Bhomia et al. (2019) in 2015. Low case letters indicate significant differences between sites. No letters are displayed in the absence of a significant difference

respectively) presumably due to floristic changes associated with perturbations (Bhomia et al. 2019), we expected faster decay rates with increasing degradation. To understand the trend observed across sites, further analysis of litter chemistry (e.g., calcium, magnesium, phosphorus, and potassium) and soil biota would need to be investigated given the important role these factors play in regulating leaf decomposition rates in tropical forests (Wieder et al. 2009; Waring 2012). Leaf litter decomposition rates at the sites (0.77 to 1.17 year<sup>-1</sup>) are in the range of global values estimated for rain forests and swamps (1.3 and 0.9 year<sup>-1</sup>, respectively; Zhang et al. 2008) but slightly higher than rates measured in peat forests of Panama (0.60–0.83 year<sup>-1</sup>; Hoyos-Santillan et al. 2015) or in palm swamp peatlands of Brazil (0.41–0.60 year<sup>-1</sup>; Sales et al. 2020). Fine root litter at the sites decomposed twice as slowly as leaf litter, with rates between 0.35 and 0.55 year<sup>-1</sup> (Dezzeo et al. 2021), confirming the importance of belowground

litter relative to aboveground litter inputs for peat accumulation in tropical systems (Chimner and Ewel 2005; Hoyos-Santillan et al. 2015).

As found in peat swamp forests of Indonesia (Jauhainen et al. 2005; Swails et al. 2019), total soil respiration (Rs) was greater in hummocks than in hollows (Fig. 3b) which is consistent with the lower WT and higher root density of hummocks versus hollows; conditions which promote both autotrophic and heterotrophic soil respiration. Rs rates fluctuated over a wide range (Fig. 3a) and remained high (~ 20 kg C ha<sup>-1</sup> day<sup>-1</sup>) in waterlogged conditions (Fig. 4b), potentially owing to oxygen availability for respiration via diffusion through the water column (Blagodatsky and Smith 2012) and respiration by aerating roots (pneumatophores) which are dense in these forests (van Lent et al. 2019). Pneumatophores facilitates aeration necessary for a variety of essential plant functions including root respiration (Colmer and Voosenek 2009). The highest Rs rate at

the Intact site (Fig. 4b) was driven by its much larger autotrophic respiration than in degraded conditions ( $5.1 \pm 1.2$  vs.  $0.4 \pm 0.9$  Mg C ha<sup>-1</sup> year<sup>-1</sup> at the Intact and degraded sites, respectively). Factors underlying such a difference include degradation-driven modifications of the soil-vegetation complex notably a reduction under degraded conditions of the size and relative area of hummocks (Table S6B) and of pneumatophore density ( $5.6 \pm 1.2$ ,  $1.9 \pm 0.6$ ,  $0.3 \pm 0.2$  pneumatophores dm<sup>-2</sup> at the Intact, mDeg, and hDeg sites, respectively; van Lent et al. 2019). Across sites, we observed an exponential decay relationship between Rs and soil moisture (Fig. 4a) which has been detected in other forests (Bowden et al. 2004) but was found to be weak in Indonesian peat swamp forests (Hergoualc'h et al. 2017a, b; Ishikura et al. 2017). Furthermore, the linear decrease in Rs rates as the WT level rises (Fig. 4b) is a trend which mirror that of previous studies conducted in Indonesian peat swamp forests of Sumatra (Comeau et al. 2013) and Kalimantan (Hergoualc'h et al. 2017b; Swails et al. 2019). The 3-year annual average Rs rates at the sites ( $6.5$ – $12.6$  Mg C ha<sup>-1</sup> year<sup>-1</sup>, Fig. 3b) are higher than values measured in Panamanian peat forests ( $4.7$ – $6.1$  Mg C ha<sup>-1</sup> year<sup>-1</sup>; Wright et al. 2013) and on the lower end of the average for undisturbed peat swamp forests of Southeast Asia ( $12.9 \pm 2.1$  Mg C ha<sup>-1</sup> year<sup>-1</sup>; Hergoualc'h and Verchot 2014).

In contrast with Rs, soil heterotrophic respiration (Rh) rates were similar at both microtopographies (Fig. 3d), as also found in an Indonesian pristine peat forest (Hergoualc'h et al. 2017b). The contrasting moisture levels between microtopographies (Fig. S5C, D) were expected to drive larger emissions in hummocks than in hollows but this effect may have been cancelled out by other differences influencing organic matter decomposition such as for instance the soil C:N ratio which tended to be higher in hummocks than in hollows (Fig. 4d). Across sites, soil heterotrophic respiration decreased linearly as the WFPS increased (Fig. 4c), in contrast with the polynomial trend with a maximum Rh around 60–70% WFPS determined from controlled in vitro conditions (van Lent et al. 2019), as also observed elsewhere (Husen et al. 2014; Linn and Doran 1984). While in situ and ex situ results agree on decreased Rh rates as the WFPS increases above 60%, below this threshold which was rare in situ (7% of observations, Fig. 4c) other factors may have constrained in situ Rh

rates such as for instance substrate availability. Microbial decomposition is largely limited by the supply of labile substrate from new detritus (Ryan and Law 2005) and soil moisture can have indirect effects on substrate diffusion and availability (Davidson et al. 2006). Concerning degradation, while medium degradation did not meaningfully alter Rh rates, heavy degradation increased the annual average rate by 28% compared to the Intact site (Fig. 3d). Soil heterotrophic respiration stems from the decomposition of litter inputs and soil organic matter (SOM), though given the lower litter inputs (Table 1) and slower litter decomposition rates (Fig. S9) at the hDeg site than in intact conditions, enhanced SOM decomposition is likely to have contributed the most to the difference in Rh rates among sites. The relationships showing a shift from the heavily degraded site to the other sites of reduced Rh rate as the peat C:N ratio, C content, and P content increased and as the peat Ca content declined (Fig. 4d–f) support this hypothesis. Furthermore, these factors have been identified elsewhere as indicators of degradation with lower peat C concentration, C:N ratio, P content and higher Ca content associated with a higher degree of peat decomposition and mineralization of SOM (Jordan et al. 2007; Könönen et al. 2015; Säurich et al. 2017; Leiffield et al. 2020). At the degraded sites, the higher mean annual Rh rates around live palms than around cut palms (Fig. 3d) suggest a greatest decomposition of recent SOM and litter than of older ones. This implies that the thick roots of stumps had already partially decomposed when measurements were performed and is evidenced by the difference in hummock size between live and cut palms, with a 25–36% smaller hummock area around stumps as compared to hummocks surrounding live palms (Table S6B). In terms of magnitude, annual average Rh rates at the Intact and mDeg sites ( $7.5 \pm 1.1$  and  $6.1 \pm 0.5$  Mg C ha<sup>-1</sup> year<sup>-1</sup>, respectively) were close to the mean for Southeast Asian pristine peat swamp forests ( $6.9 \pm 1.1$ ; Hergoualc'h and Verchot 2014) while the rate at the hDeg site ( $9.6 \pm 0.6$  Mg C ha<sup>-1</sup> year<sup>-1</sup>) was comparable to the mean for Southeast Asian degraded forested peatlands (logged, drained or affected by fire) of  $9.5 \pm 1.1$  Mg C ha<sup>-1</sup> year<sup>-1</sup> (Hergoualc'h and Verchot 2014) and to the rate in an Indonesian undrained secondary forest ( $8.2 \pm 0.7$ ; Swails et al. 2021). It is worthwhile noting that the increase in Rh from Intact to highly degraded conditions was similar to



estimates for the conversion of primary forest to undrained secondary forest including intermediary phases of slash-and-burn and crop cultivation (Swails et al. 2021) and following primary forest conversion to drained degraded forest (Hergoualc'h and Verchot 2014) in Southeast Asia.

#### Impact of forest degradation on the peat CO<sub>2</sub>-C and C budget and ecosystem C stock losses

Our research produced the first peat CO<sub>2</sub>-C and C budgets for undrained peat forests of Latin America and for undrained degraded forests in the tropics. Limitations of these estimates include their lack of spatiotemporal representativeness since they were based on a single year (when all fluxes were concomitantly monitored) at three sites. They were also computed with the assumptions of similar DOC losses regardless of degradation and of similar heterotrophic soil respiration rates of trees and hollows around palms. Since DOC concentrations are predominantly controlled by litter C mass and decomposition rate (Zhou et al. 2015), they could have differed according to degradation level. Likewise, and despite the absence of artificial drainage, the annual discharge may have varied among sites. The bias on the peat C budgets from using a single default value is however minor since the order of typical natural fluxes in undrained tropical peatlands (0.5–0.6 Mg C ha<sup>-1</sup> year<sup>-1</sup>; Drösler et al. 2014) is within the uncertainty of single components of the carbon budget (Table 1). Soil respiration of trees was monitored at the Intact site and rates were comparable to soil respiration in hollows surrounding palms [see Table 5.4 in the thesis by van Lent (2020)]. Even though these results included both autotrophic and heterotrophic respiration, they suggest minimal impact on site-scale Rh rates.

The CO<sub>2</sub>-C sink capacity of the soil in undegraded conditions ( $-1.8 \pm 1.3$  Mg C ha<sup>-1</sup> year<sup>-1</sup>) is remarkably close to the average for Southeast Asian intact peat swamp forests ( $-1.4 \pm 1.8$  Mg C ha<sup>-1</sup> year<sup>-1</sup>; Hergoualc'h and Verchot 2014) while the C sink capacity ( $-1.6 \pm 1.3$  Mg C ha<sup>-1</sup> year<sup>-1</sup>) is about two times the long-term accumulation rate ( $-0.74$  Mg C ha<sup>-1</sup> year<sup>-1</sup>) estimated for the same site (Lähteenoja et al. 2009a). The latter reflects C accumulation in peat layers below a 170 cm depth since radiocarbon dating calibration of recent superficial layers is uncertain. Our measurements on the other hand represent

an accumulation rate in the top layer and over a short period. The soil at the medium degradation site was neither a sink nor a source ( $-0.2 \pm 0.8$  Mg C ha<sup>-1</sup> year<sup>-1</sup>) with a rate similar to the long-term accumulation estimate by Lähteenoja et al. (2009a) ( $-0.4$  Mg C ha<sup>-1</sup> year<sup>-1</sup>) at a Peruvian Amazonian open herbaceous peatland where *M. flexuosa* is naturally scarce. Finally, the high peat CO<sub>2</sub>-C loss rate at the heavily degraded site ( $6.0 \pm 0.7$  Mg C ha<sup>-1</sup> year<sup>-1</sup>) is comparable with the average for Southeast Asian drained degraded peat swamp forests ( $5.3 \pm 1.6$  Mg C ha<sup>-1</sup> year<sup>-1</sup>; Hergoualc'h and Verchot 2014) and four times higher than the value reported for an Indonesian undrained secondary forest ( $1.4 \pm 1.2$  Mg C ha<sup>-1</sup> year<sup>-1</sup>; Swails et al. 2021). The simultaneous C inputs reduction and heterotrophic soil respiration increase caused by heavy degradation was more important than observations in Southeast Asia after forest drainage and degradation (Hergoualc'h and Verchot 2014) or after 30 years of forest regrowth following clearance (Swails et al. 2021). The rapidity and intensity of degradation have prompted drastic changes which magnitude and constancy in time should be monitored elsewhere. While this paper focused on the peat CO<sub>2</sub>-C and C budgets, assessing the impact of all GHG is critical to understand implications on climate change. We found no site-scale impact of degradation on soil CH<sub>4</sub> and N<sub>2</sub>O emissions (Hergoualc'h et al. 2020) and peat GHG budgets in Y2 (S10) indicate that the peat at the degraded sites was a net source of GHG. At the Intact site, the peat was neither a source nor a sink and ecosystem level CO<sub>2</sub> and CH<sub>4</sub> fluxes from 2019 (Griffis et al. 2020) combined with Y2 soil N<sub>2</sub>O emissions suggest that the forest is a GHG sink.

Destructive harvesting of forest resources at the degraded sites reduced the density of palms and trees (Table S6A). The drastic decrease in *M. flexuosa* palms at the hDeg site (81% less than the Intact site) confirms results by Hergoualc'h et al. (2017a) (89%) and Bhomia et al. (2019) (94%) elsewhere in the Pastaza-Marañón basin. The 31% and 62% biomass C stock depletion under medium and high degradation are more important than reductions observed in Peruvian palm swamps (11% and 17% for the same levels of degradation; Hergoualc'h et al. 2017a) but similar in magnitude to forest degradation impacts following logging activities and large-scale tree removal in Colombia (reduction of initial biomass C stock by 35% and 62% for moderate to high and severe

degradation; Meyer et al. 2019). However, there is very limited research on degradation of the same nature to compare with, degradation levels depend to a great extent on the intensity and frequency of disturbances, and the classification and evaluation of the degree of forest degradation relies on study-specific assessment methods (Vásquez-Grandón et al. 2018). Developing guidelines for identifying degradation levels in palm swamp peatlands based on structural, compositional and regeneration criteria is a step required for further improvement of degradation evaluation.

Medium and high degradation resulted in ecosystem C losses of 32 and 78.7 Mg C ha<sup>-1</sup> over 5 years, respectively (Table 1). While these losses are relevant, they are lower than the 143.4 Mg C ha<sup>-1</sup> estimate over 5 years due to the degradation of Southeast Asian peat swamp forests (biomass reduction of 116.9 Mg C ha<sup>-1</sup> according to Hergoualc'h and Verchot 2011, and peat emission of 26.5 Mg C ha<sup>-1</sup> as per Hergoualc'h and Verchot 2014). Assessments over longer time periods are necessary to determine to which extent biomass stocks are further reduced depending on local practices and how these could affect peat C losses. Also, investigating the interannual variability of peat C budgets would be needed to confirm the temporal trends hypothesized in this study.

## Conclusion

While anthropogenic degradation in Amazonian palm swamp forests has been a common practice for decades (Dezzeo et al. 2021; Horn et al. 2012; Virapongse et al. 2017), few studies have measured the implications on C cycling. Our results demonstrate that recurrent *M. flexuosa* destructive harvesting results in large biomass losses and turns the peat from a C sink into an important net source. Fluxes contributing to the peat C budget were more variable in time than in space and their temporal variability was closely related to moisture changes (precipitation for litterfall, water-filled pore space for soil heterotrophic respiration). These fluxes were drastically altered in highly degraded conditions (Table 1), due to reduced standing biomass for litterfall, and to enhancement of soil organic matter decomposition

for soil heterotrophic respiration. The emission factors produced in this study are essential for countries where such practices occur (e.g. Peru, Ecuador) to refine GHG estimates from forest degradation and to evaluate the potential for emission reduction through the implementation of mitigation measures. The later include the conservation and sustainable management of Amazonian peatlands dominated by *M. flexuosa* and the promotion of sustainable harvesting practices such as climbing instead of felling. This would not only maintain a sustainable population growth with sufficient recruitment of new seedlings, it would also protect the C stored in both the vegetation and the peat. Finally, our study highlights the urgent need to study the impact on GHG emissions of the degradation of tropical peat swamp forests beyond drainage, burning and conversion to other land uses as typically observed in Southeast Asia.

**Acknowledgements** We would like to extend our gratitude towards our partners at the Instituto de Investigaciones de la Amazonía Peruana (IIAP) in Iquitos, and we would especially like to thank Dr. Dennis del Castillo Torres and his team for their support. The government of Loreto is greatly acknowledged for providing access to the Quistococha Park. We would further like to thank Nicole Mitidieri Rivera for her hard work in the field, and above all this research would not have been possible without the support of the inhabitants of the villages San Julian and Las Brisas; special thanks to Ulises Mozombite Murayari for his endless effort and hard work. Finally, we are grateful to the reviewers for their insightful comments on the paper. The concept for this paper was presented at the workshop "Peatlands for climate change mitigation in agriculture" that took place in Aarhus, Denmark, on 4–5 October 2022, and which was sponsored by the Organisation for Economic Co-operation and Development (OECD) Co-operative Research Programme: Sustainable Agricultural and Food Systems. The opinions expressed and arguments employed in this publication are the sole responsibility of the authors and do not necessarily reflect those of the OECD or of the governments of its Member countries.

**Author contributions** JL, KH, LVV and JWG designed the experiment; JL, ML and JGR conducted fieldwork; JL and KH conducted the experiment; JL, KH, ND, and ML analyzed the data; all authors contributed to and approved the final manuscript.

**Funding** This research was conducted under the Sustainable Wetlands Adaptation and Mitigation Program (SWAMP) and CIFOR's Global Comparative Study on REDD+. It was generously supported by the Government of the United States of America (Grant MTO- 069018) and Government of the Norway (Grant agreement # QZA-12/0882). It was undertaken as part of the CGIAR research program on Forests, Trees

and Agroforestry (CRP-FTA) with financial support from the CGIAR Fund Donors.

**Data availability** Additional data generated as part of this study are available in the supplementary information. Raw and summary replication data are available at <https://data.cifor.org/dataset.xhtml?persistentId=doi:10.17528/CIFOR/DATA.00284>

#### Declarations

**Conflict of interest** The authors have no relevant financial or non-financial interests to disclose.

**Open Access** This article is licensed under a Creative Commons Attribution 4.0 International License, which permits use, sharing, adaptation, distribution and reproduction in any medium or format, as long as you give appropriate credit to the original author(s) and the source, provide a link to the Creative Commons licence, and indicate if changes were made. The images or other third party material in this article are included in the article's Creative Commons licence, unless indicated otherwise in a credit line to the material. If material is not included in the article's Creative Commons licence and your intended use is not permitted by statutory regulation or exceeds the permitted use, you will need to obtain permission directly from the copyright holder. To view a copy of this licence, visit <http://creativecommons.org/licenses/by/4.0/>.

#### References

- Anderson MJ (2017) Permutational multivariate analysis of variance (PERMANOVA). Wiley StatsRef: statistics reference online, ©. Wiley, Hoboken, pp 2014–2017. <https://doi.org/10.1002/9781118445112.stat07841>
- Bhomia RK, van Lent J, Rios JMG, Hergoualc'h K, Coronado ENH, Murdiyars D (2019) Impacts of *Mauritia flexuosa* degradation on the carbon stocks of freshwater peatlands in the Pastaza-Marañón river basin of the Peruvian Amazon. *Mitig Adapt Strateg Glob Change* 24:645–668
- Blagodatsky S, Smith P (2012) Soil physics meets soil biology: towards better mechanistic prediction of greenhouse gas emissions from soil. *Soil Biol Biochem* 47:78–92. <https://doi.org/10.1016/j.soilbio.2011.12.015>
- Blain D, Murdiyars D, Couwenberg J et al (2014) Rewetted organic soils. In: Hiraishi T, Krug T, Tanabe K, Srivastava N, Jamsranjav B, Fukuda M, Troxler T (eds) 2013 Supplement to the 2006 IPCC guidelines for National Greenhouse Gas Inventories: Wetlands. Intergovernmental Panel on Climate Change, Switzerland
- Blodau C (2002) Carbon cycling in peatlands—a review of processes and controls. *Environ Rev* 10:111–134. <https://doi.org/10.1139/a02-004>
- Blois JL, Williams JW, Fitzpatrick MC, Jackson ST, Ferrier S (2013) Space can substitute for time in predicting climate change effects on biodiversity. *Proc Natl Acad Sci* 110:9374–9379
- Bodmer R, Puertas P, García J, Días D, Reyes C (1999) Game animals, palms, and people of the flooded forests: management considerations for the Pacaya-Samiria National Reserve, Peru. *Adv Econ Bot* 13:217–231
- Bowden RD, Davidson E, Savage K, Arabia C, Steudler P (2004) Chronic nitrogen additions reduce total soil respiration and microbial respiration in temperate forest soils at the Harvard Forest. *For Ecol Manage* 196:43–56
- Caballero AC (2017) Aboveground biomass estimation in palm trees using terrestrial LiDAR and tree modelling. Master of Science Thesis Report GIRS-2017-05, p 55. Wageningen University and Research Centre. The Netherlands. <https://edepot.wur.nl/417823>
- Chave J, Navarrete D, Almeida S, Álvarez E, Aragão LEOC, Bonal D et al (2010) Regional and seasonal patterns of litterfall in tropical South America. *Biogeosciences* 7:43–55. <https://doi.org/10.5194/bg-7-43-2010>
- Chimner RA, Ewel KC (2005) A tropical freshwater wetland: II. production, decomposition, and peat formation. *Wetl Ecol Manag* 3:671–684
- Colmer TD, Voisenek LACJ (2009) Flooding tolerance: suites of plant traits in variable environments. *Funct Plant Biol* 36(8):665. <https://doi.org/10.1071/FP09144>
- Comeau L-P, Hergoualc'h K, Smith J, Verchot L (2013) Conversion of intact peat swamp forest to oil palm plantation: effects on soil CO<sub>2</sub> fluxes in Jambi, Sumatra. Working paper 110. CIFOR, Bogor, Indonesia. [http://www.cifor.org/publications/pdf\\_files/WPapers/WP110Comeau.pdf](http://www.cifor.org/publications/pdf_files/WPapers/WP110Comeau.pdf)
- Davidson EA, Janssens IA, Luo Y (2006) On the variability of respiration in terrestrial ecosystems: moving beyond Q10. *Glob Change Biol* 12:154–164
- Dezzeo N, Grandez-Ríos J, Martius C, Hergoualc'h K (2021) Degradation-driven changes in fine root carbon stocks, productivity, mortality, and decomposition rates in a palm swamp peat forest of the Peruvian Amazon. *Carbon Balance Manage*. <https://doi.org/10.1186/s13021-021-00197-0>
- Draper FC, Roucoux KH, Lawson IT, Mitchard ETA, Honorio Coronado EN, Lähteenoja O, Torres Montenegro L, Valderrama Sandoval E, Zaráte R, Baker TR (2014) The distribution and amount of carbon in the largest peatland complex in Amazonia. *Environ Res Lett* 9:1–12. <https://doi.org/10.1088/1748-9326/9/12/124017>
- Dröslér M, Verchot LV, Freibauer A, Pan G, Evans CD, Bourbonniere RA et al (2014) Drained inland organic soils. In: Hiraishi T, Krug T, Tanabe K, Srivastava N, Jamsranjav B, Fukuda M et al (eds) 2013 Supplement to the 2006 Guidelines for National Greenhouse Gas Inventories: Wetlands. Intergovernmental Panel on Climate Change, Switzerland
- Giweta M (2020) Role of litter production and its decomposition, and factors affecting the processes in a tropical forest ecosystem: a review. *J Ecol Environ*. <https://doi.org/10.1186/s41610-020-0151-2>
- Gonçalves RVS, Cardoso JCF, Oliveira PE, Oliveira DC (2021) Changes in the Cerrado vegetation structure: insights from more than three decades of ecological succession. *Web Ecol* 21:55–64. <https://doi.org/10.5194/we-21-55-2021>
- Graham JD, Glenn NF, Spaete LP, Hanson PJ (2020) Characterizing peatland microtopography using gradient and

- microform-based approaches. *Ecosystems* 23:1464–1480. <https://doi.org/10.1007/s10021-020-00481-z>
- Griffiths NA, Hanson PJ, Ricciuto DM, Iversen CM, Jensen AM, Malhotra A, McFarlane KJ, Norby RJ, Sargsyan K, Sebestyen SD, Shi X, Walker AP, Ward EJ, Warren JM, Weston DJ (2017) Temporal and spatial variation in peatland carbon cycling and implications for interpreting responses of an ecosystem-scale warming experiment. *Soil Sci Soc Am J* 81:1668–1688. <https://doi.org/10.2136/sssaj2016.12.0422>
- Griffis TJ, Roman DT, Wood JD, Deventer J, Fachin L, Rengifo J, Del Castillo D, Lilleskov E, Kolka R, Chimner RA, del Aguila-Pasquel J, Wayson C, Hergoualc'h K, Baker JM, Cadillo-Quiroz H, Ricciuto DM (2020) Hydrometeorological sensitivities of net ecosystem carbon dioxide and methane exchange of an Amazonian palm swamp peatland. *Agric for Meteorol*. <https://doi.org/10.1016/j.agrfor.2020.108167>
- Gumbrecht T, Roman-Cuesta RM, Verchot L, Herold M, Wittmann F, Householder E et al (2017) An expert system model for mapping tropical wetlands and peatlands reveals South America as the largest contributor. *Glob Change Biol* 23:3581–3599. <https://doi.org/10.1111/gcb.13689>
- Hastie A, Honorio Coronado EN, Reyna J et al (2022) Risks to carbon storage from land-use change revealed by peat thickness maps of Peru. *Nat Geosci* 15:369–374. <https://doi.org/10.1038/s41561-022-00923-4>
- Hergoualc'h K, Verchot LV (2011) Stocks and fluxes of carbon associated with land-use change in Southeast Asian tropical peatlands: a review. *Glob Biogeochem Cycles*. <https://doi.org/10.1029/2009GB003718>
- Hergoualc'h K, Verchot LV (2014) Greenhouse gas emission factors for land use and land-use change in Southeast Asian peatlands. *Mitig Adapt Strat Glob Change* 19:789–807. <https://doi.org/10.1007/s11027-013-9511-x>
- Hergoualc'h K, Gutiérrez-Vélez VH, Menton M, Verchot LV (2017a) Characterizing degradation of palm swamp peatlands from space and on the ground: an exploratory study in the Peruvian Amazon. *For Ecol Manage* 393:63–73. <https://doi.org/10.1016/j.foreco.2017.03.016>
- Hergoualc'h K, Hendry DT, Murdiyarso D, Verchot LV (2017b) Total and heterotrophic soil respiration in a swamp forest and oil palm plantations on peat in Central Kalimantan, Indonesia. *Biogeochemistry* 135:203–220. <https://doi.org/10.1007/s10533-017-0363-4>
- Hergoualc'h K, Carmenta R, Atmadja S, Martius C, Murdiyarso D, Purnomo H (2018) Managing peatlands in Indonesia: challenges and opportunities for local and global communities. *CIFOR Infobrief*, 205
- Hergoualc'h K, Dezzeo N, Verchot L, Martius C, van Lent J, del Aguila-Pasquel J, López M (2020) Spatial and temporal variability of soil N<sub>2</sub>O and CH<sub>4</sub> fluxes along a degradation gradient in a palm swamp peat forest in the Peruvian Amazon. *Glob Change Biol* 26:6236–6250. <https://doi.org/10.1111/gcb.15354>
- Hergoualc'h K, Maldonado-Fonken MS, Urciuolo A, Wheeler CE, Benavides JC, de Bievre B, Dominguez E, Girkin N, Hastie A, Honorio Coronado E, Infante Mata D, Iturraspe R, Izquierdo AE, Lawson I, León C, Lilleskov E, Malpica-Piñeros C, Rodríguez Martínez AC, Pancotto V, Pérez Quezada J, Ribeiro K, Silva AC (2022) Regional Assessment for Latin America and the Caribbean. In: *GlobalPeatlands Initiative* (ed) *Global peatlands assessment—the state of the world's peatlands: evidence for action toward the conservation, restoration, and sustainable management of peatlands*. Main report. United Nations Environment Programme, Nairobi, pp 155–191
- Hidalgo Pizango CG, Honorio Coronado EN, del Aguila-Pasquel J, Flores Llampazo G, de Jong J, Córdova Oroche CJ, Reyna Huaymacari JM, Carver SJ, del Castillo Torres D, Draper FC, Phillips OL, Roucoux KH, de Bruin S, Peña-Claros M, van der Zon M, Mitchell G, Lovett J, García Mendoza G, Gatica Saboya L, Irarica Pacaya J, Brañas MM, Ramírez Paredes E, Baker TR (2022) Sustainable palm fruit harvesting as a pathway to conserve Amazon peatland forests. *Nat Sustain* 5:479–487. <https://doi.org/10.1038/s41893-022-00858-z>
- Horn CM, Gilmore MP, Endress BA (2012) Ecological and socio-economic factors influencing aguaje (*Mauritia flexuosa*) resource management in two indigenous communities in the Peruvian Amazon. *For Ecol Manage* 267:93–103. <https://doi.org/10.1016/j.foreco.2011.11.040>
- Horn CM, Vargas Paredes VH, Gilmore MP, Endress BA (2018) Spatio-temporal patterns of *Mauritia flexuosa* fruit extraction in the Peruvian Amazon: Implications for conservation and sustainability. *Appl Geogr* 97:98–108. <https://doi.org/10.1016/J.APGEOG.2018.05.004>
- Hoyos-Santillan J, Lomax BH, Large D, Turner BL, Boom A, Lopez OR, Sjögersten S (2015) Getting to the root of the problem: litter decomposition and peat formation in lowland neotropical peatlands. *Biogeochemistry* 126:115–129. <https://doi.org/10.1007/s10533-015-0147-7>
- Husen E, Salma S, Agus F (2014) Peat emission control by groundwater management and soil amendments: evidence from laboratory experiments. *Mitig Adapt Strat Glob Change* 19:821–829. <https://doi.org/10.1007/s11027-013-9526-3>
- IBM Corp (2017) IBM SPSS Statistics for Windows. Version 25.0. IBM Corp, Armonk, NY
- Ishikura K, Yamada H, Toma Y et al (2017) Effect of groundwater level fluctuation on soil respiration rate of tropical peatland in Central Kalimantan, Indonesia. *Soil Sci Plant Nutr* 63:1–13
- Jauhainen J, Takahashi H, Heikkinen JEP, Martikainen PJ, Vasander H (2005) Carbon fluxes from a tropical peat swamp forest floor. *Glob Change Biol* 11:1788–1797. <https://doi.org/10.1111/j.1365-2486.2005.01031.x>
- Jordan S, Veltz S, Zeitz J (2007) The influence of degree of peat decomposition on phosphorus binding forms in fens. *Mires Peat* 2:7
- Kerdraon D, Drewer J, Chung AYC, Majalap N, Slade EM, Bréchet L, Wallwork A, Castro-Trujillo B, Sayer EJ (2020) Litter inputs, but not litter diversity, maintain soil processes in degraded tropical forests—a cross-continental comparison. *Front for Glob Change*. <https://doi.org/10.3389/ffgc.2019.00090>
- Könönen M, Jauhainen J, Laiho R et al (2015) Physical and chemical properties of tropical peat under stabilised land uses. *Mires Peat* 16:8



- Kozłowski TT (1997) Responses of woody plants to flooding and salinity. *Tree Physiol* 17:490–490. <https://doi.org/10.1093/treephys/17.7.490>
- Krishna MP, Mohan M (2017) Litter decomposition in forest ecosystems: a review. *Energy Ecol Environ* 2:236–249
- Laiho R (2006) Decomposition in peatlands: reconciling seemingly contrasting results on the impacts of lowered water levels. *Soil Biol Biochem* 38:2011–2024
- Lähteenoja O, Ruokolainen K, Schulman L, Oinonen M (2009a) Amazonian peatlands: an ignored C sink and potential source. *Glob Change Biol* 15:2311–2320. <https://doi.org/10.1111/j.1365-2486.2009.01920.x>
- Lähteenoja O, Ruokolainen K, Schulman L, Alvarez J (2009b) Amazonian floodplains harbour minerotrophic and ombrotrophic peatlands. *CATENA* 79:140–145. <https://doi.org/10.1016/J.CATENA.2009.06.006>
- Lähteenoja O, Rojas Reátegui Y, Räsänen M, Del Castillo Torres D, Oinonen M, Page S (2012) The large Amazonian peatland carbon sink in the subsiding Pastaza-Marañón foreland basin, Peru. *Glob Change Biol* 18:164–178. <https://doi.org/10.1111/j.1365-2486.2011.02504.x>
- Leiffield J, Klein K, Wüst-Galley C (2020) Soil organic matter stoichiometry as indicator for peatland degradation. *Sci Rep* 10:7634. <https://doi.org/10.1038/s41598-020-64275-y>
- Lilleskov E, McCullough K, Hergoualc'h K, del Castillo Torres D, Chimner R, Murdiyarso D et al (2019) Is Indonesian peatland loss a cautionary tale for Peru? A two-country comparison of the magnitude and causes of tropical peatland degradation. *Mitig Adapt Strateg Glob Change* 24:591–623. <https://doi.org/10.1007/s11027-018-9790-3>
- Linn DM, Doran JW (1984) Effect of water-filled pore space on carbon dioxide and nitrous oxide production in tilled and nontilled soils. *Soil Sci Soc Am J* 48:1267–1272
- Lo E (2005) Gaussian error propagation applied to ecological data: post-ice-storm-downed woody biomass. *Ecol Monogr* 75:451–466. <https://doi.org/10.1890/05-0030>
- Marengo J (1998) Climatología de la zona de Iquitos, Perú. In: Kalliola R, Flores Paitán S (eds) *Geoecología y desarrollo amazónico: estudio integrado en la zona de Iquitos, Perú*. *Annales Universitatis Turkuensis Ser A II* 114. University of Turku, Finland, pp 35–57
- Meyer V, Saatchi S, Ferraz A, Xu L, Duque A, García M, Chave J (2019) Forest degradation and biomass loss along the Chocó region of Colombia. *Carbon Balance Manage*. <https://doi.org/10.1186/s13021-019-0117-9>
- Mishra BP, Tripathi OP, Tripathi RS, Pandey HN (2004) Effects of anthropogenic disturbance on plant diversity and community structure of a sacred grove in Meghalaya, northeast India. *Biodivers Conserv* 13:421–436
- Murdiyarso D, Kauffman JB, Verchot LV (2013) Climate change mitigation strategies should include tropical wetlands. *Carbon Manage* 4:491–499. <https://doi.org/10.4155/Cmt.13.46>
- Ong CSP, Juan JC, Yule CM (2015) Litterfall production and chemistry of *Koompassia malaccensis* and *Shorea uliginosa* in a tropical peat swamp forest: plant nutrient regulation and climate relationships. *Trees* 29:527–537. <https://doi.org/10.1007/s00468-014-1130-y>
- Padoch C (1988) Aguaje (*Mauritia flexuosa* L.f.) in the economy of Iquitos, Peru. *Adv Econ Bot* 6:214–224
- Penn J, van Sledright M, Bertiz Torres G, Guerra Soplín E (2008) Los aguajales y sus condiciones en el Río Tahuayo: Aportes para el Plan Maestro del Área de Conservación Regional Comunal Tamshiyacu-Tahuayo (ACRCTT). Programa de conservación, gestión y uso sostenible de la diversidad biológica en la región Loreto (PROCREL), Iquitos, Perú
- Pezeshki SR (2001) Wetland plant responses to soil flooding. *Environ Exp Bot* 46:299–312. [https://doi.org/10.1016/S0098-8472\(01\)00107-1](https://doi.org/10.1016/S0098-8472(01)00107-1)
- Core Team R (2017) R: A language and environment for statistical computing. <https://www.R-project.org/>
- Roucoux KH, Lawson IT, Jones TD, Baker TR, Coronado ENH, Gosling WD, Lähteenoja O (2013) Vegetation development in an Amazonian peatland. *Palaeogeogr Palaeoclimatol Palaeoecol* 374:242–255. <https://doi.org/10.1016/j.palaeo.2013.01.023>
- Ryan MG, Law BE (2005) Interpreting, measuring, and modeling soil respiration. *Biogeochemistry* 73:3–27
- Sales BG, Lessa TAM, Freitas DA, Veloso MDM, Silva MLS, Fernandes LA, Frazão LA (2020) Litterfall dynamics and soil carbon and nitrogen stocks in the Brazilian palm swamp ecosystems. *For Ecosyst*. <https://doi.org/10.1186/s40663-020-00251-2>
- Säurich A, Tiemeyer B, Don A, Bechtold M, Amelung W, Freibauer A (2017) Vulnerability of soil organic matter of anthropogenically disturbed organic soils. *Biogeosci Discuss* 2017:1–33
- Seneviratne SI, Nicholls N, Easterling D, Goodess CM, Kanae S, Kossin J et al (2012) Changes in climate extremes and their impacts on the natural physical environment. In: Field CB, Barros V, Stocker TF, Qin D, Dokken DJ, Ebi KL et al (eds) *Managing the risks of extreme events and disasters to advance climate change adaptation, a special report of working groups I and II of the Intergovernmental Panel on Climate Change (IPCC)*. Cambridge University Press, Cambridge. <https://doi.org/10.2134/jeq2008.0015br>
- Seta T, Demissew S, Woldu Z (2018) Litterfall dynamics in Boter-Becho forest: moist evergreen montane forest of Southwestern Ethiopia. *J Ecol Nat Environ* 10:13–21
- Swails E, Hergoualc'h K, Verchot L, Novita N, Lawrence D (2021) Spatio-temporal variability of peat CH<sub>4</sub> and N<sub>2</sub>O fluxes and their contribution to peat GHG budgets in Indonesian forests and oil palm plantations. *Front Environ Sci* 9:1–15
- Swails E, Hertanti D, Hergoualc'h K, Verchot L, Lawrence D (2019) The response of soil respiration to climatic drivers in undrained forest and drained oil palm plantations in an Indonesian peatland. *Biogeochemistry* 142:37–51. <https://doi.org/10.1007/s10533-018-0519-x>
- Tonin AM, Gonçalves JF Jr, Bambi P, Couceiro SRM, Feitoza LAM, Fontana LE, Hamada N et al (2017) Plant litter dynamics in the forest stream interface: Precipitation is a major control across tropical biomes. *Sci Rep*. <https://doi.org/10.1038/s41598-017-10576-8>
- van Lent J (2020) Land-use change and greenhouse gas emissions in the tropics: forest degradation on peat soils. PhD dissertation, Wageningen University



- van Lent J, Hergoualc'h K, Verchot L, Oenema O, van Groenigen JW (2019) Greenhouse gas emissions along a peat swamp forest degradation gradient in the Peruvian Amazon: soil moisture and palm roots effects. *Mitig Adapt Strateg Glob Change* 24:625–643. <https://doi.org/10.1007/s11027-018-9796-x>
- Vásquez-Grandón A, Donoso PJ, Gerding V (2018) Forest degradation: when is a forest degraded? *Forests* 9:726. <https://doi.org/10.3390/f9110726>
- Virapongse A, Endress BA, Gilmore MP, Horn C, Romulo C (2017) Ecology, livelihoods, and management of the *Mauritia flexuosa* palm in South America. *Glob Ecol Conserv* 10:70–92. <https://doi.org/10.1016/j.gecco.2016.12.005>
- Waring BG (2012) A meta-analysis of climatic and chemical controls on leaf litter decay rates in tropical forests. *Ecosystems* 15:999–1009. <https://doi.org/10.1007/s10021-012-9561-z>
- Wieder WR, Cleveland CC, Townsend AR (2009) Controls over leaf litter decomposition in wet tropical forests. *Ecology* 90:3333–3341. <https://doi.org/10.1890/08-2294.1>
- Wright EL, Black CR, Turner BL, Sjögersten S (2013) Environmental controls of temporal and spatial variability in CO<sub>2</sub> and CH<sub>4</sub> fluxes in a neotropical peatland. *Glob Change Biol* 19:3775–3789. <https://doi.org/10.1111/gcb.12330>
- Zhang D, Hui D, Luo Y, Zhou G (2008) Rates of litter decomposition in terrestrial ecosystems: global patterns and controlling factors. *J Plant Ecol* 1:85–93
- Zhang H, Yuan W, Dong W, Liu S (2014) Seasonal patterns of litterfall in forest ecosystem worldwide. *Ecol Complex* 20:240–247
- Zhou W-J, Sha L-Q, Schaefer DA, Zhang Y-P, Song Q-H, Tan Z-H, Deng Y, Deng X-B, Guan H-L (2015) Direct effects of litter decomposition on soil dissolved organic carbon and nitrogen in a tropical rainforest. *Soil Biol Biochem* 81:255–258

**Publisher's Note** Springer Nature remains neutral with regard to jurisdictional claims in published maps and institutional affiliations.